Article

On the Mechanism of the cis-trans Isomerization in the Lowest Electronic States of Azobenzene: S0, S1, and T1

CEMBRAN, Alessandro, *et al*.

Abstract

In this paper, we identify the most efficient decay and isomerization route of the S1, T1, and S0 states of azobenzene. By use of quantum chemical methods, we have searched for the transition states (TS) on the S1 potential energy surface and for the S0/S1 conical intersections (CIs) that are closer to the minimum energy path on the S1. We found only one TS, at 60° of CNNC torsion from the E isomer, which requires an activation energy of only 2 kcal/mol. The lowest energy CIs, lying also 2 kcal/mol above the S1 minimum, were found on the torsion pathway for CNNC angles in the range 95−90°. The lowest CI along the inversion path was found ca. 25 kcal/mol higher than the S1 minimum and was characterized by a highly asymmetric molecular structure with one NNC angle of 174°. These results indicate that the S1 state decay involves mainly the torsion route and that the inversion mechanism may play a role only if the molecule is excited with an excess energy of at least 25 kcal/mol with respect to the S1 minimum of the E isomer. We have calculated the spin−orbit couplings between S0 and T1 at several geometries along the [...]

Reference

CEMBRAN, Alessandro, *et al*. On the Mechanism of the cis-trans Isomerization in the Lowest Electronic States of Azobenzene: S0, S1, and T1. *Journal of the American Chemical Society*, 2004, vol. 126, no. 10, p. 3234-3243

DOI : 10.1021/ja038327y

J|A|C|S
ARTICLES
Published on Web 02/21/2004

On the Mechanism of the cis−trans Isomerization in the Lowest Electronic States of Azobenzene: S_0, S_1, and T_1

Alessandro Cembran,† Fernando Bernardi,† Marco Garavelli,*,†
Laura Gagliardi,‡ and Giorgio Orlandi*,†,§

Contribution from the Department of Chemistry "G. Ciamician", University of Bologna, Bologna, Italy, the Department of Physical Chemistry "F. Accascina", University of Palermo, Palermo, Italy, and INSTM, University of Bologna, Bologna, Italy

Received September 4, 2003; E-mail: marco.garavelli@unibo.it; gorlandi@ciam.unibo.it

Abstract: In this paper, we identify the most efficient decay and isomerization route of the S_1, T_1, and S_0 states of azobenzene. By use of quantum chemical methods, we have searched for the transition states (TS) on the S_1 potential energy surface and for the S_0/S_1 conical intersections (CIs) that are closer to the minimum energy path on the S_1. We found only one TS, at 60° of CNNC torsion from the E isomer, which requires an activation energy of only 2 kcal/mol. The lowest energy CIs, lying also 2 kcal/mol above the S_1 minimum, were found on the torsion pathway for CNNC angles in the range 95−90°. The lowest CI along the inversion path was found ca. 25 kcal/mol higher than the S_1 minimum and was characterized by a highly asymmetric molecular structure with one NNC angle of 174°. These results indicate that the S_1 state decay involves mainly the torsion route and that the inversion mechanism may play a role only if the molecule is excited with an excess energy of at least 25 kcal/mol with respect to the S_1 minimum of the E isomer. We have calculated the spin−orbit couplings between S_0 and T_1 at several geometries along the CNNC torsion coordinate. These spin−orbit couplings were about 20−30 cm^{-1} for all the geometries considered. Since the potential energy curves of S_0 and T_1 cross in the region of twisted CNNC angle, these couplings are large enough to ensure that the T_1 lifetime is very short (∼10 ps) and that thermal isomerization can proceed via the nonadiabatic torsion route involving the $S_0-T_1-S_0$ crossing with preexponential factor and activation energy in agreement with the values obtained from kinetic measures.

1. Introduction

Azobenzene (Ab) can exist in two forms, namely, the cis (Z) and trans (E) isomers, which can interconvert both photochemically and thermally.[1−3] Since the two isomers exhibit well-separated absorption bands in the UV−visible region and different physical properties, such as dielectric constant and refractive index, Ab and its derivatives are good candidates for many applications such as light-triggered switches,[4] constituents of erasable holographic data, image storage devices and materials with photomodulable properties,[5−8] and as a possible basis for a light-powered molecular machine.[8] For these reasons, the photophysical and photochemical properties of Ab have been and still are the subject of a widespread interest.[1−3,9−25]

The low-energy absorption spectrum of Ab shows a weak band in the visible and an intense band in the near UV spectral region. In hexane solution of the E isomer at room temperature, the former shows a maximum at 432 nm (ϵ_{max} = 400 L mol^{-1} cm^{-1}) and the latter shows a maximum at 318 nm (ϵ_{max} =

† Department of Chemistry "G. Ciamician", University of Bologna.
‡ University of Palermo.
§ INSTM, University of Bologna.

(1) Zimmermann, G.; Chow, L. Y.; Park, U. I. *J. Am. Chem. Soc.* **1958**, *80*, 3528.
(2) (a) Fischer, E. *J. Am. Chem. Soc.* **1960**, *82*, 3249. (b) Fischer, E.; Malkin, S. *J. Phys. Chem.* **1962**, *66*, 2482.
(3) Rau, H.; Luddeke, E. *J. Am. Chem. Soc.* **1982**, *104*, 1616.
(4) Rau, H. In *Photocromism, Molecules and Systems*; Dürr, H., Bounas-Laurent, H., Eds.; Elsevier: Amsterdam, 1990; Vol. 1, Chapter 4, pp 165−192.
(5) Ikeda, T.; Tsutsumi, O. *Science* **1995**, *268*, 1873.
(6) (a) Willner, I.; Rubin, S.; Riklin, A. *J. Am. Chem. Soc.* **1995**, *113*, 3321. (b) Shipway, A. N.; Willner, I. *Acc. Chem. Res.* **2001**, *34*, 421.
(7) Liu, Z. F.; Hashimoto, K.; Fujishima, K. *Nature* **1990**, *347*, 658.
(8) (a) Balzani, V.; Credi, A.; Marchioni, F.; Stoddard, J. F. *Chem. Commun.* **2001**, 1860. (b) Ballardini, R.; Balzani, V.; Credi, A.; Gandolfi, M. T.; Venturi, M. *Acc. Chem. Res.* **2001**, *34*, 445. (c) Balzani, V.; Credi, A.; Venturi, M. *Coord. Chem. Rev.* **1998**, *171*, 3.
(9) Hugel, T.; Holland, N. B.; Cattani, A.; Moroder, L.; Seitz, M.; Gaub, H. E. *Science* **2002**, *296*, 1103.
(10) Griffiths, J. *Chem. Soc. Rev.* **1972**, *1*, 41.
(11) Rau, H. *Angew. Chem., Int. Ed. Engl.* **1973**, *12*, 224.
(12) Lednev, I.; Ye, T. Q.; Matousek, P.; Townie, M.; Foggi, P.; Neuwahl, F.; Umapathy, S.; Hester R.; Moore, J. *Chem. Phys. Lett.* **1998**, *290*, 68.
(13) Nagële, T.; Hoche, R.; Zinth, W.; Wachtveitl, J. *J. Chem. Phys.* **1997**, *106*, 519.
(14) Lednev, I.; Ye, T. Q.; Hester R.; Moore, J. *J. Phys. Chem.* **1996**, *100*, 13338.
(15) Hochstrasser, R. M.; Lower, S. K. *J. Chem. Phys.* **1962**, *36*, 3505.
(16) Dick, R. H.; McClure, D. S. *J. Chem. Phys.* **1962**, *36*, 2326.
(17) Bortolus, P.; Monti, S. *J. Phys. Chem.* **1979**, *83*, 648.
(18) Siampiringue, N.; Guyot, G.; Bortolus, P.; Monti, S. *J. Photochem.* **1987**, *37*, 185.
(19) Rau, H. *J. Photochem.* **1984**, *26*, 221.
(20) Monti, S.; Orlandi, G.; Palmieri, P. *Chem. Phys.* **1982**, *71*, 87.
(21) Cattaneo, P.; Persico, M. *Phys. Chem. Chem. Phys.* **1999**, *1*, 4739.
(22) Fujino, T.; Arzhantsev, S. Yu.; Tahara, T. *J. Phys. Chem. A* **2001**, *105*, 8123.
(23) Ishikawa, T.; Noro, T.; Shoda, T. *J. Chem. Phys.* **2001**, *115*, 7503.
(24) (a) Schultz, T.; Quenneville, J.; Levine, B.; Toniolo, A.; Martinez, T. J.; Lochbrunner, S.; Schmitt, M.; Shaffer, J. P.; Zgierski, M. Z.; Stolow, A. *J. Am. Chem. Soc.* **2003**, *125*, 8098. (b) Stolow, A. *Annu. Rev. Phys. Chem.* **2003**, *54*, 89.
(25) Gagliardi, G.; Orlandi, G.; Bernardi, F.; Cembran, A.; Garavelli, M. *Theor. Chem. Acc.*, in press.

 10.1021/ja038327y CCC: $27.50

22 300 L mol^{-1} cm^{-1}).[4,10−14] The former band is structureless even in low-temperature mixed crystals[15,16] and is attributed to the lowest singlet state, S_1, of nπ^* nature and of B_g type in the C_{2h} symmetry group. The $S_1 \leftarrow S_0$ transition is then symmetry-forbidden and becomes allowed when the molecule is distorted along an a_u coordinate, such as the (properly symmetrized) twistings around CN bonds. The second band, which shows a rich vibronic structure with the origin at 362 nm (27 662 cm^{-1}) in spectra measured in dibenzyl single crystal at 20 K,[16] is attributed to the state S_2, of $\pi\pi^*$ nature and of B_u symmetry type. Thus, while the $S_1 \leftarrow S_0$ transition is symmetry-forbidden, the $S_2 \leftarrow S_0$ transition is allowed in analogy with the $S_1 \leftarrow S_0$ transition in stilbene. In the Z azobenzene (*Z*-Ab) isomer, one finds two similar bands in the UV−visible absorption spectrum, at 440 and 260 nm, with similar intensity ratio as in *E*-Ab.[4]

An important and still not understood property of the Z−E photoisomerization of Ab is the dependence of the quantum yield of this process on the excitation wavelength.[1−4] In an inert solvent such as *n*-hexane, the quantum yields of the E → Z photoconversion are 0.25 and 0.12 exciting the S_1 and S_2 states,[17] respectively. The quantum yields of the inverse process Z → E are 0.53 and 0.40 exciting the S_1 and S_2 states, respectively.[17,18] Very similar quantum yields are found in other solvents.[3,19] This violation of the Kasha rule implies that S_2 decays to the ground state, bypassing the FC region of the S_1 state, at least partially.

The violation of the Kasha rule disappears in sterically hindered azobenzenes, for example, in azobenzenophanes (Ab-phanes), where the motion of each Ab molecule is somewhat affected by the companion molecule.[3,4] Similar results were found in an azobenzene-capped crown ether.[19]

While in stilbene and in ethylene derivatives the Z−E isomerization can occur only via torsion of the C═C bond, in Ab it can proceed along two pathways: the torsion around the N═N double bond and the in-plane inversion. In the latter case, the transition state corresponds to a linear geometry whereby one nitrogen atom is sp hybridized.

The traditional interpretation[3,4] has assigned the isomerization on the S_1 and the S_2 states to different paths, namely to the inversion and the torsion paths, respectively. Assuming that in sterically hindered Ab the torsion motion is frozen, an explanation was provided for the different S_1 and S_2 isomerization quantum yields observed only in Ab and not in Ab-phanes. An early[20] and a more recent and refined[21] quantum chemical study as well as the time-resolved photophysical studies of Lednev and co-workers[12,14] provided support to this mechanism.

Very recently, new theoretical and experimental results have questioned this model. Tahara and co-workers[22] have proposed, on the basis of new time-resolved fluorescence data and their interpretation, that the isomerization occurs for both S_1 and S_2 excited states through the inversion coordinate. On the theoretical side, Ishikawa et al.[23] have calculated at the multiconfiguration level the potential energy surfaces (PES) of the lowest singlet excited states and found that these favor the torsion pathway. Stolow et al., on the basis of combined time-resolved photoelectron spectroscopy observations and ab initio calculations,[24] have associated the non-Kasha behavior of the Ab photoisomerization with the quasi-degeneracy between the benzenic states and the S_2 state localized on the azo group. Clearly, our understanding of a very complex process such as the Ab photoisomerization is still unsatisfactory.

In a recent contribution,[25] we have studied in detail the role of the torsion coordinate in the deactivation of the lowest electronic states of Ab by the density functional theory (DFT) at the B3LYP[26] level and by complete active space SCF (CASSCF) calculations, followed by second-order perturbation theory corrections (CASPT2).[27]

In the ground state, we found that the optimized barrier for isomerization is ca. 40 kcal/mol higher than the optimized E isomer for both inversion and torsion pathways. According to B3LYP calculations, the optimized PES of T_1 along the torsion pathway has its minimum at roughly 105° where its energy is 28.0 kcal/mol.[25] This implies that, provided that the S_0-T_1 spin−orbit (SO) coupling is sufficiently strong, thermal isomerization can occur via the T_1 state by overcoming a barrier of about 32 kcal/mol, corresponding to the higher S_0-T_1 crossing.

The isomerization on T_1 was found to show a strong preference for the torsion route: at the B3LYP level, the optimized energies at the twisted and inverted geometry were found to be 28.0 and 48.4 kcal/mol, respectively.[25] Thus, the Ab molecule, once it is excited in T_1 at the E or Z geometry, follows the torsion pathway, reaching the minimum where it crosses to S_0 thereby giving isomerization.

In this work, we present a detailed study of the S_0, S_1, and T_1 PES in the isolated Ab molecule and find the minimum energy paths (MEP), the transition state (TS), and the S_1-S_0 conical intersections (CIs) leading to the S_1 deactivation and to the E−Z photoisomerization. From the energies and the locations of CIs, we can show that torsion is the most important coordinate for the Ab photoisomerization and explains the short lifetime of S_1. CIs connected with the inversion pathway have also been detected, but these are much higher in energy to represent an appreciable deactivation channel of S_1. Furthermore, we present the results of calculations of S_0-T_1 SO interactions and find that they are large enough to justify the short lifetime of T_1 and to suggest that the nonadiabatic torsion route involving the $S_0-T_1-S_0$ crossing is the most plausible candidate for the thermal isomerization. A reaction scheme is presented, highlighting the preferred isomerization pathways for Ab in the S_0, T_1, and S_1 states, which provides a fully consistent interpretation of experimental results.

2. Computational Details

The PES for the E−Z thermal- and photoisomerization has been studied using fully unconstrained optimizations and MEP computations at the CASSCF level,[27] followed by single-point CASPT2[27] computations on the optimized relevant structures to account for correlation energy. A state average CASSCF procedure, with equal weights for the S_1 and S_0 states, has been used to generate molecular orbitals and the reference functions for subsequent CASPT2 calculations. All these computations have been performed using the Gaussian 98 package[28] and the MOLCAS-5.2 quantum chemistry program.[29]

The active space choice is a crucial step in a CASSCF calculation. After a series of tests it turned out that a balanced active space was 14 electrons in 12 orbitals (14/12), corresponding to the 10/10 π valence and the two doubly occupied nitrogen lone pairs. In the C_{2h} group of symmetry, the π orbitals belonged to the A_u and B_g irreducible

(26) (a) Becke, A. D. *J. Chem. Phys.* **1993**, *98*, 5648. (b) Lee, C.; Yang, W.; Parr, R. G. *Phys. Rev. B* **1988**, *37*, 785.
(27) Roos, B. O. In *Ab Initio Methods in Quantum Chemistry II*; Lawley, K. P., Ed.; Advances in Chemical Physics Series 69; John Wiley & Sons: Chichester, England, 1987; p 399.

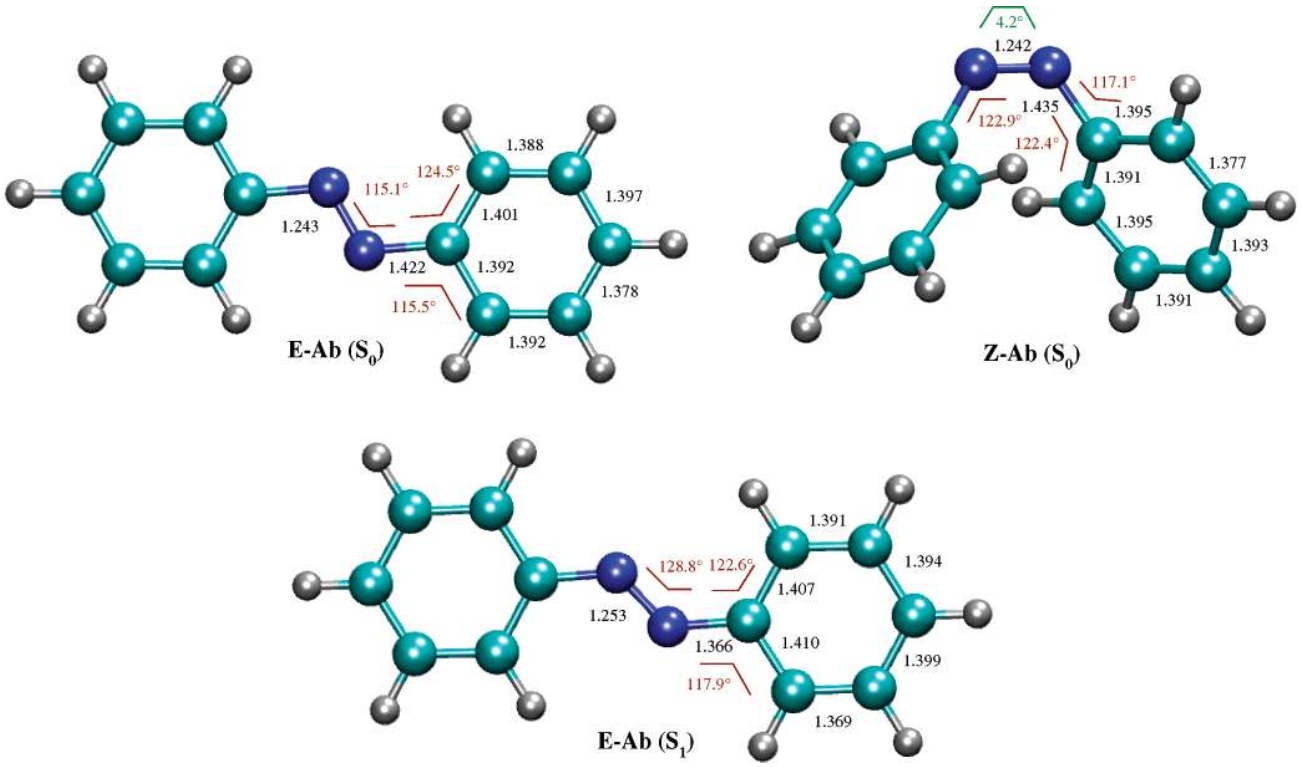

Figure 1. Azobenzene-optimized stationary points: S_0 minimum for *E*-Ab (*E*-Ab(S_0)), S_0 minimum for *Z*-Ab (*Z*-Ab(S_0)), and S_1 minimum for *E*-Ab (*E*-Ab(S_1)). Bond lengths (black numbers) are in angstroms, and CNN and CCN bending angles (red numbers) and CCNN and CNNC dihedral angles (green numbers) are in degrees.

representations. Most of the 14/12 calculations were performed with an active space composed by 1, 1, 5, and 5 active orbitals in the four irreducible representations A_g, B_u, A_u, and B_g, respectively. This active space corresponded to the nitrogens π and π^*, their two lone pairs, and eight benzenic orbitals (the two most occupied and the two less occupied benzenic orbitals were excluded). A 6-31G* basis set of atomic orbitals was used in this case. Some computations were also performed using a different set of 14/12 active space orbitals, comprising six and four active π orbitals in the A_u and B_g irreducible representations, respectively, and using a generally contracted basis sets of atomic natural orbital (ANO) with the contraction scheme 3s2p1d on C and N and 2s1p on H.[30] These two alternative approaches yielded substantially similar results and, unless differently specified, we will refer to the first type of computations.

The effects of SO coupling were introduced using a newly developed method based on the CASSCF state interaction approach (CASSI).[31,32] Here, the CASSCF wave function generated for the S_0 and T_1 states were allowed to mix under the influence of a spin−orbit Hamiltonian. The method has recently been described,[33] and we refer to this article for details. In these calculations, the ANO basis set and the second active space choice were used.

The search for CIs was performed by using procedures developed in our laboratory or according to the prescriptions of ref 34.

3. Results

A. Analysis of the S_1 PES and Determination of S_0−S_1 Conical Intersections. The optimized geometries of the E isomer in the S_0 and S_1 singlet states and of the ground-state Z isomer, calculated at the 14e/12o CASSCF level of the theory, are reported in Figure 1. A minimum in the S_1 PES corresponding to the Z isomer does not exist, and in Figure 1 only the Z form ground-state geometry is shown.

In both electronic states the E isomer is planar, while the Z isomer is nonplanar as the C−N bonds are rotated by 62.0° and the N═N bond is rotated by 4.2° to decrease the H···H nonbonded interactions. The energy gap between the two ground-state isomers is 12.0 kcal/mol, in good agreement with the measured enthalpy difference.[35] The calculated bond lengths and angles for both isomers, which are shown in Figure 1, are in agreement with the values obtained in previous theoretical[36−38]

(28) Frisch, M. J.; Trucks, G. W.; Schlegel, H. B.; Scuseria, G. E.; Robb, M. A.; Cheeseman, J. R.; Zakrzewski, V. G.; Montgomery, J. A., Jr.; Stratmann, R. E.; Burant, J. C.; Dapprich, S.; Millam, J. M.; Daniels, A. D.; Kudin, K. N.; Strain, M. C.; Farkas, O.; Tomasi, J.; Barone, V.; Cossi, M.; Cammi, R.; Mennucci, B.; Pomelli, C.; Adamo, C.; Clifford, S.; Ochterski, J.; Petersson, G. A.; Ayala, P. Y.; Cui, Q.; Morokuma, K.; Malick, D. K.; Rabuck, A. D.; Raghavachari, K.; Foresman, J. B.; Cioslowski, J.; Ortiz, J. V.; Stefanov, B. B.; Liu, G.; Liashenko, A.; Piskorz, P.; Komaromi, I.; Gomperts, R.; Martin, R. L.; Fox, D. J.; Keith, T.; Al-Laham, M. A.; Peng, C. Y.; Nanayakkara, A.; Gonzalez, C.; Challacombe, M.; Gill, P. M. W.; Johnson, B. G.; Chen, W.; Wong, M. W.; Andres, J. L.; Head-Gordon, M.; Replogle, E. S.; Pople, J. A. *Gaussian 98*, revision A.6; Gaussian, Inc.: Pittsburgh, PA, 1998.
(29) Andersson, K.; Barysz, M.; Bernhardsson, A.; Blomberg, M. R. A.; Carissan, Y.; Cooper, D. L.; Cossi, M.; Fleig, T.; Fülscher, M. P.; Gagliardi, L.; de Graaf, C.; Hess, B. A.; Karlström, G.; Lindh, R.; Malmqvist, P.-Å.; Neogrády, P.; Olsen, J.; Roos, B. O.; Schimmelpfennig, B.; Schütz, M.; Seijo, L.; Serrano-Andrés, L.; Siegbahn, P. E. M.; Stålring, J.; Thorsteinsson, T.; Veryazov, V.; Wierzbowska, M.; Widmark, P.-O. *MOLCAS*, version 5.2; Department of Theoretical Chemistry, Chemistry Center, University of Lund: Lund, Sweden, 2001.
(30) Pierloot, K.; Dumez, B.; Widmark, P.-O.; Roos, B. O. *Theor. Chim. Acta* **1995**, *90*, 87.
(31) Malmqvist, P.-A. *Int. J. Quantum Chem.* **1986**, *30*, 479.
(32) Malmqvist, P.-A.; Roos, B. O. *Chem. Phys. Lett.* **1989**, *155*, 189.
(33) Malmqvist, P.-A.; Roos, B. O.; Schimmelpfenning, B. *Chem. Phys. Lett.* **2002**, *357*, 230.
(34) (a) Ragazos, I. N.; Robb, M. A.; Bernardi, F.; Olivucci, M. *Chem. Phys. Lett.* **1992**, *197*, 217. (b) Bearpark, M. J.; Robb, M. A.; Schlegel, H. B. *Chem. Phys. Lett.* **1994**, *223*, 269.
(35) Adamson, A. W.; Vogler, A.; Kunkely, H.; Wachter, R. *J. Am. Chem. Soc.* **1978**, *100*, 1300.
(36) Hättig, C.; Hald, K. *Chem. Phys. Phys. Chem.* **2002**, *4*, 2111.
(37) Biswas, N.; Umpathy, S. *J. Phys. Chem. A* **1997**, *101*, 5555.
(38) Fliegl, H.; Kohn, A.; Hattig, C.; Alrichs, R. *J. Am. Chem. Soc.* **2003**, *125*, 9821.

Table 1. CASPT2 and CASSCF Energies for Minima, Transition States, and Conical Intersections for the PES of S_0 and S_1 States of Azobenzene[a,b]

		CASPT2ΔE[b]		CASSCFΔE[b]	
structure	state	eV	kcal/mol	eV	kcal/mol
E-Ab (S_0)	S_0	0.00	0.0	0.00	0.0
	S_1	2.50	57.7	3.18	73.4
	T_1[c]	1.83	42.3	1.73	39.9
Z-Ab (S_0)[d]	S_0	0.52	11.9	0.71	16.4
	S_1	3.23	74.4	4.09	94.4
	T_1[c]	2.20	50.7	2.12	48.9
Ab(T_1)	S_0[c]	1.37	31.7	1.71	39.5
	T_1[c]	1.25	28.8	1.30	29.9
E-Ab (S_1)	S_0	0.70	16.1	0.69	16.0
	S_1	1.95	44.9	2.61	60.1
$TS_{tors}(S_0)$	S_0[c]	1.65	38.1	1.80	41.5
	S_1[c]	2.56	59.0	3.01	69.5
$TS_{tors}(S_1)$	S_0	1.32	30.5	1.53	35.3
	S_1	2.02	46.7	2.75	63.5
CI_{tors-1}	S_0	2.03	46.7	2.63	60.7
	S_1	2.04	47.1	2.51	57.9
CI_{tors-2}	S_0	2.00	46.2	2.57	59.3
	S_1	2.15	49.5	2.45	56.6
CI_{tors-3}	S_0	2.19	50.5	2.90	66.8
	S_1	2.36	54.5	2.96	68.3
CI_{inv}	S_0	3.00	69.1	3.70	85.4
	S_1	3.18	73.4	3.62	83.5

[a] For convenience, T_1 energies from previous work[c] are shown. [b] The energy for the ground state of the E form, chosen as the zero, is −570.90605 au at the CASPT2 level and −569.21779 au at the CASSCF level. [c] From ref 25. The energy for the ground state of the E form, chosen as the zero, is −571.04534 au at the CASPT2 level and −569.266151 au at the CASSCF level. [d] The oscillator strength *f* is 0.0118 for the $S_0 \rightarrow S_1$ transition.

and experimental work.[39−41] The optimized E structure in the S_1 singlet state is planar and shows some changes in bond lengths and bond angles with respect to S_0 (see Figure 1). In particular, the N=N bond length is slightly increased from 1.243 to 1.253 Å, and the two CN bonds are shortened considerably from 1.422 to 1.366 Å. Furthermore, a large increase from 115.1 to 128.8° of the NNC angles is observed, and this change is presumably related to the decreased electron charge in the N lone pairs in the state S_1.

The vertical $\Delta E(S_1-S_0)$ of *E*-Ab calculated at the CASPT2 level for the S_0 equilibrium geometry is 2.50 eV (see Table 1). This energy corresponds approximately to the maximum of the $S_1 \leftarrow S_0$ absorption band, which is observed at 432 nm, i.e., 2.87 eV.[4,10−14] The vertical (S_1-S_0) energy gap calculated at the S_1 equilibrium geometry, which can be associated with the maximum of the fluorescence band, is only 1.25 eV. It should be noted that the fluorescence spectrum is modulated not only by the Franck−Condon (FC) factor, but also by the ν^3 factor.[42] The observed spectral maximum occurs at the energy of 1.86 eV,[22] which differs from the calculated value (1.25 eV). This discrepancy may be due to the ν^3 factor and possibly also to the inaccuracy of the experimental measure due to the lower sensitivity of the experimental apparatus in the red wing of the spectrum.

The energy gap between the minima of the S_1 and S_0 PES, which should correlate with the 0−0 bands of fluorescence and absorption spectra (provided the zero-point energy of S_1 and S_0 is the same), is 1.95 eV according to the CASPT2 calculation. Experimentally, this energy difference can be estimated to be roughly 2.36 eV from the work of Tahara et al.[22] The difference among the energy of the absorption maximum and the energy of the 0−0 band, amounting to 0.55 eV according to the calculation and to 0.51 eV according to the spectra,[22] indicates that a sizable reorganization energy occurs upon S_1 excitation. This corresponds to the vibrational energy available in the S_1 state when the excitation wavelength corresponds to the maximum of the absorption band. From the S_1 and S_0 equilibrium structures reported above, it appears that this vibrational energy is accepted predominantly by the CN stretching and the NNC bending modes.

All the relevant electronic energies, calculated at the CASPT2 and CASSCF level, are reported in Table 1.

To analyze the dynamics and the photophysical properties of Ab excited on the S_1 state, we searched for transition states on the S_1 PES and for S_1/S_0 conical intersections that were close to the S_1 MEP. We then calculated the energies of these critical geometries at the CASPT2 level.

The potential energy curve of S_1 along the CNNC torsion obtained in recent calculations is substantially flat.[23,25] In the present work, we found that the S_1 MEP follows the torsion coordinate in the full E−Z interval. We detected only one TS, placed along the torsion coordinate between E and the twisted geometry, labeled $TS_{tors}(S_1)$, at the CNNC angle of 119.7°, that is, ca. 30° before the twisted (90°) structure. This TS is only 2 kcal/mol above the minimum of the S_1 PES, corresponding to the E isomer and, thus, is easily accessible at room temperature because of the small amount of activation energy it requires. The molecular structure of this TS is shown in Figure 2. Interestingly, the molecule has lost all its symmetry elements: the two NNCC angles are −14.3 and −9.3°, respectively, while the NNC angles are 128.9 and 125.2°, respectively. It appears that, as the CNNC torsion increases, the coupling between the two nitrogen lone-pairs weakens and the $n\pi^*$ excitation tends to localize predominantly on one moiety because of the electron−phonon coupling, that is, of the reorganization energy associated with the excitation. Therefore, the two moieties become inequivalent.

The computed S_1 MEP starting from the Z isomer follows the torsion coordinate and reaches the twisted geometry without encountering any barrier.

The lowest energy S_1/S_0 CIs are found for CNNC angles around 90° and have roughly the same energy as the transition state (see Table 1). This finding confirms the results obtained by Ishikawa et al.,[23] who constructed the two-dimensional PES of the lowest electronic states as a function of the CNNC torsion and of an NNC bending angle, optimizing only five geometrical parameters, and found that S_1 and S_0 are almost degenerate for CNNC = 90°. We have identified several CIs that belong to the section of the CI hyperline of the twisted region. Coming from the E isomer, the first CI encountered, labeled CI_{tors-1}, is characterized by the CNNC twisting angle of 94.4° and is 2 kcal/mol higher in energy than the E isomer. A second CI is found at the CNNC angle of 84.4°, a little tilted toward the Z form. This CI, labeled CI_{tors-3}, is about 5 kcal/mol above the S_1 minimum. Several CIs connect CI_{tors-1} to CI_{tors-3}, and we

(39) Brown, C. J. *Acta Chrystallogr.* **1966**, *21*, 146.
(40) Bowstra, J. A.; Schouten, A.; Kroon, J. *Acta Chrystallogr., Sect. C* **1983**, *39*, 1121.
(41) Tsuji, T.; Takashima, H.; Takeuchi, H.; Egawa, T.; Konaka, S. *J. Phys. Chem. A* **2001**, *105*, 9347.
(42) Birks, J. B. *Photophysics of Aromatic Molecules*; Wiley: London, 1970; Chapter 4.

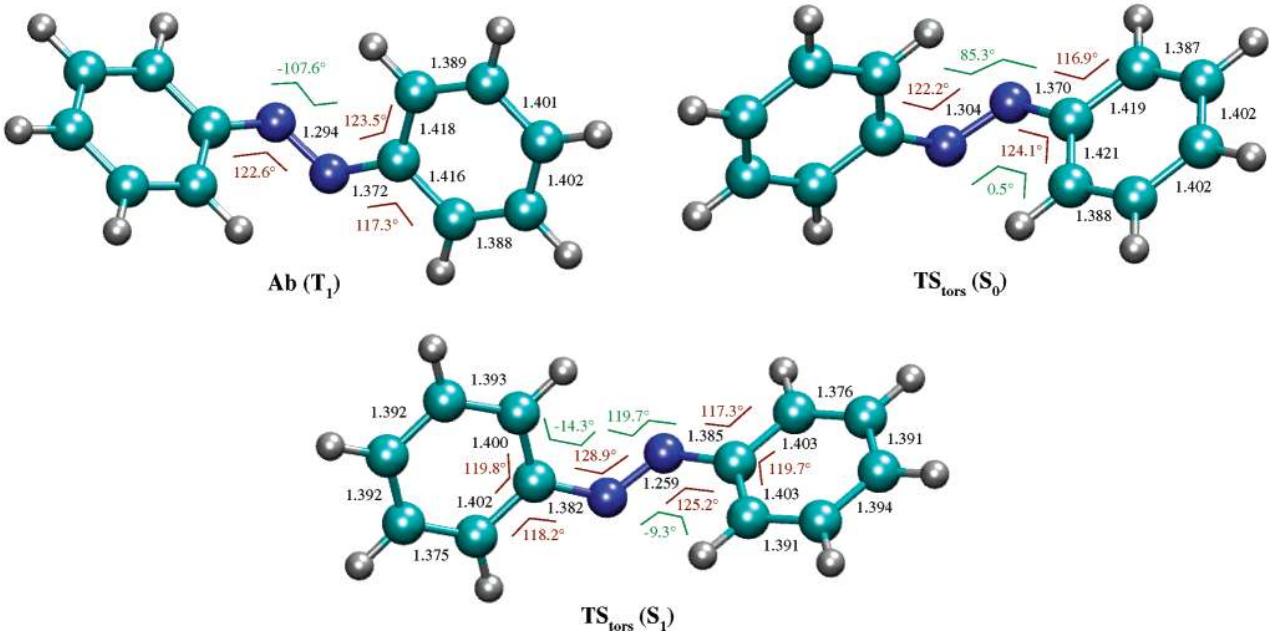

Figure 2. Structures for the azobenzene transition states in the S_0 state ($TS_{tors}(S_0)$) and in the S_1 state ($TS_{tors}(S_1)$) and for the T_1 minimum ($Ab(T_1)$). Bond lengths and bond angles are described in Figure 1.

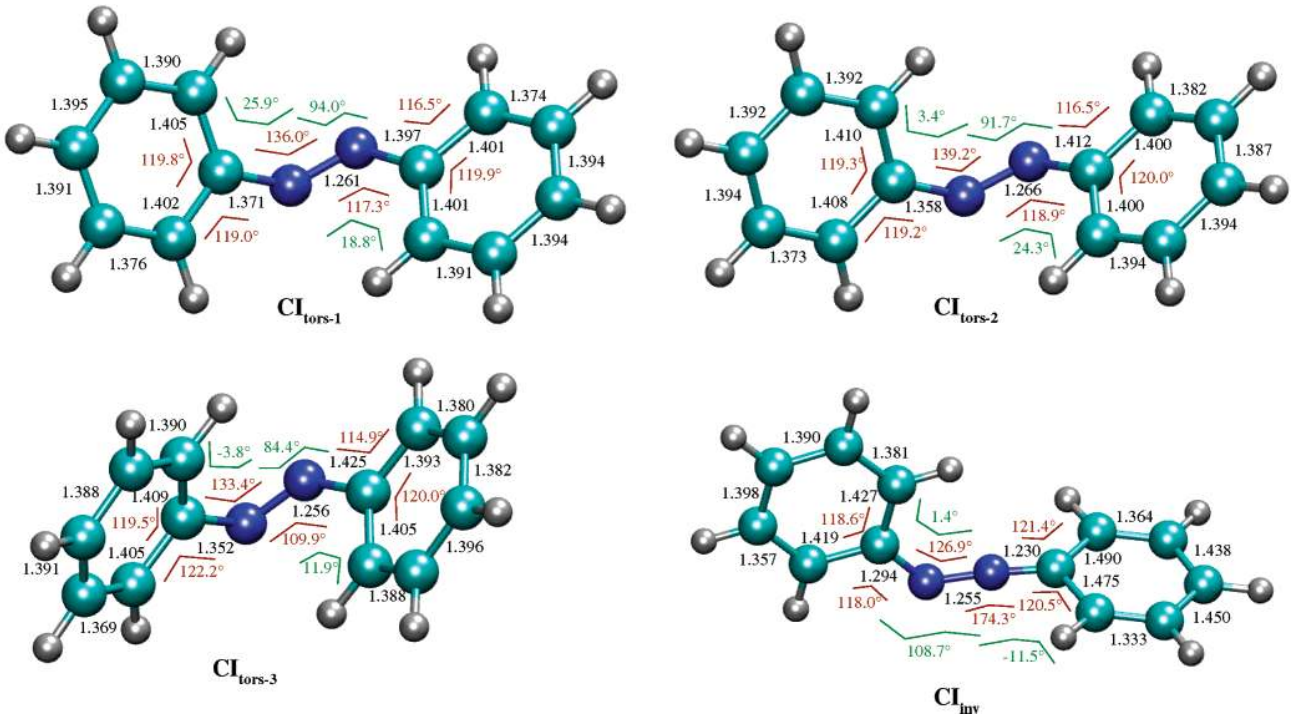

Figure 3. Structures for the azobenzene S_1/S_0 conical intersections: CI_{tors-1}, CI_{tors-2}, and CI_{tors-3} are CIs along the CNNC torsion coordinate with CNNC = 94.4, 84.4 and 91.7°, respectively. CI_{inv} is a CI along the inversion coordinate with CNN = 174.3°. Bond lengths and bond angles are described in Figure 1.

can document, for example, a CI at the CNNC angle of 91.7°, labeled CI_{tors-2}, and essentially degenerate with CI_{tors-1}.

The structure of CI_{tors-1}, which is shown in Figure 3, is quite asymmetric: the two CN bonds are 1.371 and 1.397 Å long, respectively, and the two CNN angles are 136.0 and 117.3°, respectively. The $n\pi^*$ excitation resides predominantly on the moiety where the NNC angle is larger, i.e., 136°; this large angle indicates that the NN and the CN bonds are based on nitrogen σ orbitals of intermediate sp/sp^2 hybridization, while the lone pair acquires an increased p character. On the other hand, in the moiety where the NNC angle is equal to 117°, the lone pair of the N atom remains approximately an sp^2 orbital. A similar structure is obtained for CI_{tors-2}: the NNC angles are 139.2 and 118.9°, and the full structure is shown in Figure 3. The molecular structure of CI_{tors-3}, which is also displayed in Figure 3, is even more evidently asymmetric. The CN bonds are 1.352 and 1.425 Å long, and the CNN angles are 133.4 and 109.9°.

All the three CIs reported above belong to the same $S_1(n\pi^*)/S_0$ crossing region. The S_1 state is based predominantly (see Supporting Information, Section 2) on the singly excited configuration $n\pi^*$ along the entire torsion coordinate. Obviously, the definition of n orbitals as distinct from π orbitals is strictly correct only for planar geometries. In the context of twisted structures, the n orbital is just the molecular orbital (MO) that correlates with the true n orbital at the planar geometry shown in Figure S1 of the Supporting Information. The n and the π^* orbitals, which are respectively the HOMO and LUMO in the twisted region, are shown in Figure S2 of the Supporting Information. They extend only in the NN region and are asymmetric.

In a previous paper,[25] using geometries optimized for the ground state, we found a deep twisted minimum associated with a state based on the $n^2\pi^{*2}$ configuration. Here, we have also verified that the fully optimized $n^2\pi^{*2}$ state still shows a deep minimum at the twisted geometry, but remains roughly 10 kcal/mol higher than $S_1(n\pi^*)$.

The CI_{tors-i} are easily reached from any vibrational level of S_1 because of their small activation energy, and thus, they contribute to the very fast deactivation and to the short lifetime of S_1. Since they are close to the twisted geometry, the torsion mechanism plays an important role in the S_1 decay and the associated photoisomerization. The excited Z form, which is at higher energy than the excited E isomer, can decay substantially through CI_{tors-3}, which is the first to be encountered along the computed MEP after a barrierless path.

We have searched also for S_1/S_0 CIs in the region of the inverted geometry and we have found a CI, labeled CI_{inv}, in which one of the two NNC angles is close to 180°. The molecular structure of this CI, which is shown in Figure 3, is highly asymmetric: the NNC angles are 174.3 and 126.9°, respectively, and the NC bonds are 1.230 and 1.294 Å, respectively. The CNNC dihedral angle is 108.7°. The CI_{inv} is far away from the S_1 MEP and is at a considerably higher energy than the CI_{tors-i}, about 25 kcal/mol above the S_1 minimum. Thus, it is not expected to affect appreciably the photophysical and photochemical properties of Ab. Also in the inverted region, the S_1 state is based on the n(HOMO)−π^*(LUMO) singly excited configuration. However, as is shown in Figure S3 of the Supporting Information, these MOs extend also on the benzene rings, and each of them involves a different moiety of the molecule.

Remarkably, all the CIs of the twisted and of the inverted region appear to belong to the same hyperline of the CIs. In fact, we have detected a number of CIs in the region between the CI_{tors-i} and CI_{inv}, all of them characterized by the CNNC angle close to 90° and one of the NNC angles between 180 and 130°. In particular, we have computed (see Figure 4) the MEP in the hyperline of the CIs and connecting the inverted structure CI_{inv} to the twisted region: along this MEP, the Ab molecule smoothly changes its structure from the high-energy inverted crossing (CI_{inv}) to the low-energy pure torsion points (CI_{tors-i}), still preserving the S_1/S_0 degeneracy. As an example, one of these CIs is characterized by CNNC = 93° and NNC = 127 and 151° and is 11 kcal/mol above the E isomer. Relevance and implications of this extended hyperline region (spanning structures going from the pure torsional to the inversion mechanism) in the photochemistry of Ab will be discussed in the next section.

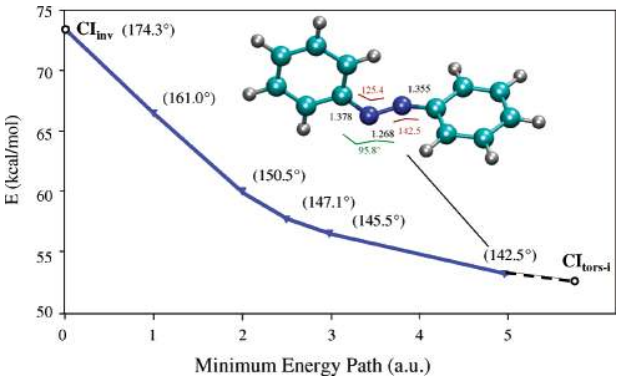

Figure 4. CASSCF fully optimized minimum energy path computed in the S_1/S_0 intersection space and connecting the high-energy CI_{inv} with the low-energy twisted region (CI_{tors-i}). The energies have been corrected by single-point CASPT2 computations. The origin of the energies is given by the ground state *trans*-azobenzene isomer (*E*-Ab) energy. Reaction coordinate is in mass weighted atomic units (au). The smoothly changing NNC bending angle is reported in brackets, while the CNNC torsion remains substantially unchanged (ca. 90°).

Interestingly, according to the present calculations, the symmetry lowering inherent to the inverted structure is associated with a substantial CNNC twisting that weakens the coupling between the two moieties of the molecule.

A picture of the MEPs computed on the S_1 PES, which follow the torsion coordinate, together with the critical geometries discussed above is presented in Figure 5.

We wish to discuss briefly the reasons why CI_{tors-i} occurs at much lower energies than CI_{inv}. From our calculations, upon excitation on S_1, the N−N bond is slightly stretched, while the N−C bonds are compressed (becoming similar to double bonds) and NNC angles open from 115 to 128°. Rotation around N−N does not significantly change the S_1 energy, because the loss of p−p interaction of the N atoms is compensated by the n−p interaction, and the NNC angles and CN bond lengths change very little. On the contrary, the energy of the ground state increases very much with the NN torsion because N−N double bond energy is substantially lost and the changes of CN bond lengths and CNN angles have the same effect. This leads to S_1/S_0 degeneration at the N−N twisted geometry at an energy close to the S_1 minimum. On the other hand, the inversion of one CNN angle in S_1 is accompanied by a large decrease of one CN bond length and a chinoid deformation of one benzene ring and brings about a significant energy increase. The energy of S_0 undergoes an even larger energy increase with the inversion of one CNN angle. Correspondingly, the energy of CI_{inv} occurs at higher energy than CI_{tors}.

B. S_0-T_1 Spin−Orbit Interactions and Intersystem Crossing. According to CASPT2 calculations,[25] the S_0 potential energy curve along the CNNC coordinate shows a barrier of 38.1 kcal/mol while the T_1 potential energy curve presents a minimum of 28.8 kcal/mol in the twisted region. The molecular structure at the T_1 minimum is shown in Figure 2, and a qualitative picture of the S_0 and T_1 potential energy curves is shown in Figure 5. The two curves cross each other at 68 and 105° of CNNC twisting. The energy of the former crossing, which is closer to the Z form, is the higher and amounts to 32 kcal/mol. According to B3LYP calculations,[25] at the inverted

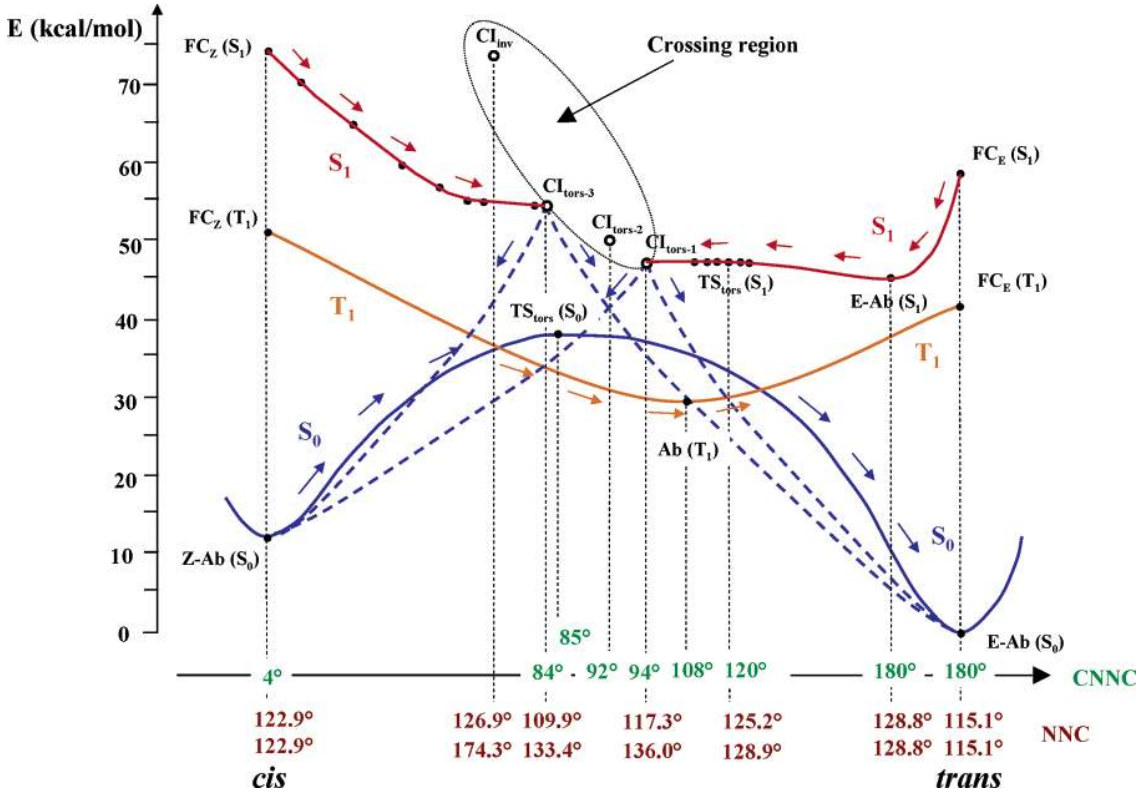

Figure 5. Singlet (S_0 and S_1) and triplet (T_1) reaction paths (i.e., MEPs) for the E → Z isomerization in azobenzene. Energy profiles are schematized for sake of clarity and have been scaled to match CASPT2 values. Open circles represent S_1/S_0 CI. The horizontal axis represents the CNNC torsion coordinate (green numbers). Values for NNC angles are also reported (brown numbers). The shaded region highlights the S_1/S_0 crossing space and embraces the low-energy (i.e., torsion) and high-energy (i.e., inversion) deactivation funnels. The paths of T_1 and S_1 radiationless decays are also shown.

geometry the energy of the S_0 barrier is 40.5 kcal/mol and the T_1 energy is 48.4 kcal/mol. The two energy curves along the inversion do not cross. Thus, the Ab molecule can easily cross from S_0 to T_1, or vice versa, in the twisted region, but not in the inverted region. The rate, k, of this intersystem crossing (isc) process, occurring at the S_0/T_1 crossings, is determined by the size of the S_0-T_1 spin−orbit coupling, V_{so}, according to the Fermi golden rule[43]

$$k = (4\pi^2/h)V_{so}^2\rho F$$

where ρ is the density of active vibrational states of the final electronic state and F is the FC factor. To evaluate k, we evaluated the S_0-T_1 SO coupling at several values of the torsion angle, optimizing the remaining structural parameters in the S_0 state, following refs 31−33. At any chosen geometry, the S_0 singlet interacts with two spin components of T_1, while the coupling with the third component is zero. This follows from the molecular symmetry, since the x, y spin components transform as B in the C_2 symmetry group (B_g in C_{2h}), the z spin component transforms as A in C_2 (A_g in C_{2h}), and the T_1 and S_0 electronic wave functions belong to the B (B_g) and A (A_g), respectively. The calculated SO couplings for the x and y spin component are complex numbers, and their moduli are reported in Table 2. The values of these couplings range from 32.4 cm^{-1} (for CNNC = 180°, i.e., the E structure) to 17.2 cm^{-1} (for CNNC = 80°).

Table 2. Spin−Orbit Interactions (V_{so}) between S_0 and a Spin Component of T_1 for Different Values of the CNNC Angle

CNNC (deg)	180	120	105	100	90	80	70	68	60
V_{so}(cm^{-1})	32.4	25.1	22.8	22.1	22.3	17.2	19.6	19.8	20.3

For our purpose, the V_{so} values obtained at 68 and 105° CNNC angles at which the $S_0 \rightarrow T_1$ or $T_1 \rightarrow S_0$ processes occur are the most relevant. The corresponding values, 19.8 and 22.8 cm^{-1}, are much larger than the typical values, less than 1 cm^{-1}, of the SO couplings between ground and $^3\pi\pi^*$ states in planar aromatic compounds.[44] This is due to the large one-center terms that contribute to V_{so} when the T_1 state has nπ^* character, as is the case of the azobenzene T_1.

The ρ can be taken as the inverse of the frequency of the vibration associated with the largest displacement in the S_0-T_1 transition and contributes more to the FC factor.[44] From the DFT calculations of S_0 and T_1 equilibrium geometries and normal coordinates[25] and vibrational assignments,[45] the most important vibration is the NC stretching characterized by a frequency of ca. 1200 cm^{-1}.

For simplicity, in our calculation we approximate the V_{so} coupling to 20 cm^{-1}. The FC factor at the S_0/T_1 crossing is relatively large, i.e., between 0.1 and 1. To obtain a qualitative estimate of the $T_1 \rightarrow S_0$ isc rate, we have chosen for F the intermediate value 0.4. In this way, the rate of the isc process between one of the T_1 active components and S_0 is 1.5 × 10^{11} s^{-1}.

(43) (a) Fermi, E. *Notes on Quantum Mechanics*; The University of Chicago Press: Chicago, 1981. (b) Fano, U. *Phys. Rev. B* **1988**, *37*, 785. (c) Robinson, G. W.; Frosch, R. P. *J. Chem. Phys.* **1962**, *37*, 1962.

(44) Henry, B. H.; Siebrand, W. In *Organic Molecular Photophysics*; Birks, J. B., Ed.; Wiley: London, 1973; Vol. 1, Chapter 2.

(45) Gruger, A.; LeCalve, N.; Dizabo, P. *J. Chim. Phys.* **1972**, *69*, 291.

Assuming that the three components of the triplet states are equally populated, the rate of the $T_1 \rightarrow S_0$ process is readily found to be 10^{11} s^{-1}. The corresponding lifetime of 10 ps, which is very short for a T_1 state, provides an explanation for the lack of spectroscopic observation of the T_1 state of Ab.

The rate of the inverse $S_0 \rightarrow T_1$ process, leading from S_0 to the two coupled components of the state T_1, is 3×10^{11} s^{-1}. Note that this rate is the same size of the preexponential factors reported for the thermal Z−E isomerization of Ab (1.95×10^{11} s^{-1} from ref 3 and 8×10^{10} s^{-1} from ref 46). These findings support the idea that the thermal isomerization of Ab can proceed by the torsion mechanism via the $S_0-T_1-S_0$ nonadiabatic path involving the triplet state. Moreover, the calculated activation energy is also consistent with the measured kinetic parameter. In fact, since our calculated energy of the higher S_0-T_1 crossing is 32 kcal/mol and the energy of the Z isomer is 12 kcal/mol, the resulting activation energy for the Z → E process is 20 kcal/mol. This value is in good agreement with the activation enthalpy of 22 kcal/mol measured for the thermal isomerization.[3,46]

Interestingly, Talaty and Fargo,[47] who originally mentioned this proposal, rejected it because they considered the measured preexponential factor to be too high for a spin-forbidden process. Therefore they supported, as other authors,[48] the inversion mechanism because they estimated the torsion barrier on the S_0 energy curve to be about 50 kcal/mol, that is, much higher than the experimental value.

4. Discussion and Conclusion

The main purpose of this work is to identify the most efficient decay and isomerization route of the S_1 state of Ab. By use of quantum chemical methods, we have searched for the transition states leading from the E and Z excited isomers to the funnels determining the decay of S_1. We have also identified the MEPs on the S_1 PES and the CIs that are closer to them, which are generally the most relevant for the decay and the photophysical and photochemical properties of Ab. The results are summarized in Figure 5.

The MEP is found to follow the torsion coordinate. The only TS we could find is characterized by CNNC = 119.7° (see Figure 2) and requires an activation energy of 2 kcal/mol. Thus, the exit from the minimum of the S_1 PES, i.e., the excited E isomer, toward the isomerization must involve a twisting of ca. 60° of the N═N bond. The lowest energy S_0/S_1 CIs, lying just 2 kcal/mol above the S_1 minimum, are found at twisted geometries with the CNNC angle in the range of 95−90°. At these geometries the molecule has lost its symmetry, in particular the two NNC angles have become different, with the larger NNC angle amounting to 136°.

To assess the role of the inversion coordinate in the decay process and in the photoisomerization mechanism in S_1, we have searched for CIs along this coordinate. We found that the lowest CI in the inversion region, with one of the NNC angles of 174.3°, is ca. 25 kcal/mol higher than the S_1 minimum. Other CIs with the larger NNC angle varying between 174 and 130°, and with the CNNC angle always close to 90°, were detected (see Figure 4).

These results indicate clearly that for both E and Z isomers the S_1 state decay involves mainly the torsion route. On the contrary, the mechanism based only on the inversion route, requiring the activation energy of about 25 kcal/mol, can play only a negligible role. It may be operative only provided that the molecule has an excess vibrational energy of at least 25 kcal/mol, but even in this case, the rapid energy redistribution among the various vibrations renders the concentration of such amounts of energy in the inversion coordinate very unlikely, and thus, the inversion mechanism becomes inefficient. In the case of vertical excitation of the Z isomer, the Ab molecule has enough vibrational energy to reach the CI_{inv}, but, as pointed out, the rapid vibrational energy redistributions make the decay via the CIs of the twisted region a much more likely choice also because they are easily reached by a barrierless path.

To determine quantitatively the E−Z isomerization quantum yields, a more complete characterization of the S_1 PES around these CIs and molecular dynamical simulations are required. At a qualitative level, the barrierless versus the barrier-controlled twisting path accounts for the observed higher yield of the Z → E, with respect with the E → Z, photoisomerization process.

It is worthwhile to note that the inversion mechanism, in which one NNC angle opens up to 180° while the other remains approximately at 120°, implies the loss of molecular symmetry. This can occur only if the two N-ϕ moieties of Ab become decoupled because of the weakening of their interaction. In our calculations, we have noted that the molecular symmetry disappears at the molecular geometries where the CNNC angle is twisted by at least 60°. In particular, the opening of the NNC angle is found always associated with the CNNC twisting of ca. 90°. This indicates that a simple way to achieve the decoupling of the two N-ϕ moieties is to apply a degree of torsion around the N═N bond, because it weakens the conjugation between the two moieties. This implies that the inversion mechanism cannot operate alone, but needs to be combined and induced by a significant amount of torsion. On the other hand, the torsion mechanism by itself can lead to an easy E−Z isomerization. If we take into account not only geometric paths, but also the activation energies, the possible pathways for the S_1 photoisomerization are not simply torsion or inversion, but rather, they may be distinguished as follows:

(a) Simple torsion around the N═N bond, which is the most favored on energy ground,

(b) Torsion around the N═N bond combined with some degree of inversion of one NNC angle. In this case, the activation energies increase with the opening of the NNC angle, and

(c) Inversion mechanism, which is the limiting case of (b), when NNC reaches 180°.

To clarify further the interplay of the inversion mechanism with the torsion coordinate, we have mapped the CI hyperline connecting the CIs of the twisted region with the CIs of the inverted region. These results (see Figure 4) show that an extended S_1/S_0 crossing region exists which embraces structures smoothly changing from a pure torsional (lower energy) to an inversion (higher energy by ca. 25 kcal/mol) mechanism. This feature is shown to be of high chemical relevance for Ab S_1 photochemistry: S_1 reaction channels for the isolated molecule (i.e., the MEPs shown in Figure 5), both from the cis and trans Ab side, are seen to intercept the low energy part of the intersection space, thus pointing unambiguously to a favored

(46) Brown, E. V.; Grunneman, G. R. *J. Am. Chem. Soc.* **1975**, *97*, 621.
(47) Talaty, E. R.; Fargo, J. C. *J. Chem. Soc., Chem. Commun.* **1967**, 65.
(48) Asano, T.; Okada, T.; Shinkai, S.; Shigematsu, K.; Kusano, Y.; Manabe, O. *J. Am. Chem. Soc.* **1981**, *103*, 5161.

torsional reaction coordinate as the intrinsic photoisomerization path for isolated Ab on S_1. Nevertheless, if the pure twisting motion is hindered for some reason and a space saving photoisomerization process is preferred (for example, for Ab molecules inserted in liquid crystal stacked layers or in the solid state), a compromise between energetic and geometric requirements can be possibly reached, favoring deactivation funnels at geometries intermediate between pure torsional and inversion mechanisms. In these cases, assigning the photoisomerization process to a pure reaction coordinate (either torsion or inversion) can be misleading, and both components can become important.

The present results, as well as recent previous work,[23,25] contradict the traditional notion that the photoisomerization of isolated Ab in the $S_1(n\pi^*)$ state occurs via the inversion coordinate. This idea is based on the observation that in Ab-phanes, at variance with Ab, the quantum yields of photoisomerization in S_1 and S_2 are the same[3] and are qualitatively equal to the quantum yield of Ab in S_1. It is based also on the assumption that the E−Z isomerization via torsion of one Ab molecule belonging to Ab-phanes would be inhibited by the rigidity of the system, which would prevent large sweeping motion of the benzene rings. However, this argument is not supported by an estimate of the energy penalty for isomerization via rotation of one Ab molecule in Ab-phanes. As a matter of fact, the Ab-phanes, which allow one *E*-Ab (11 Å long from one para carbon atom to the other) to coexist with one *Z*-Ab (only 7 Å long), cannot be very rigid. The modest rigidity of the Ab-phanes, and the weakness of the argument, is demonstrated by the experiments of Tanner and Wennerstrom[49] who were able to show that even the stilbenophanes, for which the inversion coordinate is not available, do isomerize. The present results are in contrast with the inversion mechanism proposed by Tahara el al.[22] on the basis of their time-resolved measures of fluorescence spectra and decay kinetics. Their analysis originates from arbitrary assumptions about the mechanism and the geometry of singlets decay that are not supported by the observations or theoretical arguments. Therefore, the torsion mechanism for the E−Z isomerization on S_1 does not seem to be contrasted by any clear-cut experimental evidence.

The present results provide an explanation for the observed time dependence of the S_1 fluorescence and $S_n \leftarrow S_1$ transient absorption. The fluorescence emission was found to decay with a lifetime of 0.3 ps in the E form and 0.1 ps in the Z form.[50] A similar lifetime, 0.2 ps, was found recently[51] for the E isomer excited in the S_1 state. The transient absorption was found to decay with a biexponential form with time constants of 0.3 and 3 ps in the E form and, according to a single-exponential way, with a time constant of 0.1 ps in the Z form.[50] We attribute the subpicosecond decay of fluorescence and of the transient absorption to the vibrational energy redistribution starting from the FC excited vibronic states. We associate the slower decay (3 ps) of the transient absorption observed only for the E isomer with the subsequent motion toward the CIs of the twisted region, which requires the overcoming of a barrier of 2 kcal/mol and is thereby slower. The barrierless path leading from the Z form to the twisted CIs on the S_1 PES agrees with the absence of the slow component observed in the Z isomer decay. To the best of our knowledge, the only measures of the E−Z photoisomerization in Ab as a function of the temperature (*T*) were performed by Fischer.[2] They show that, by exciting S_1, the Z → E quantum yields are essentially independent of *T*, while the E → Z quantum yields decrease by lowering *T* in such a way as to suggest the activation energy to be 2 kcal/mol, a value in very good agreement with the TS_{tors-1} energy calculated by us (see Table 1).

In this work, we provide evidence in support of the torsion mechanism for the Ab isomerization in the states S_0 and T_1. As is shown in Figure 5, the minimum in the T_1 PES is found at the twisted geometry, where it is below the S_0 barrier. The ground singlet state PES has a TS of similar energies, ca. 40 kcal/mol, for both the isomerization routes. However, the S_0 and T_1 PES cross along the torsion, but not along the inversion coordinate. Therefore, the decay of T_1 is expected to occur more efficiently via the torsion mechanism, and its rate depends on the strength of the relevant SO couplings. We have now found that these couplings, amounting to about 20 cm^{-1}, are large enough to ensure that the rate of the $T_1 \rightarrow S_0$ isc process is of the order of 10^{11} s^{-1}. This rate indicates that Ab can decay from T_1 to the ground state in ca. 10 ps and that the torsion mechanism provides indeed a very efficient mechanism for the T_1 decay and isomerization. The short T_1 lifetime and, presumably, the difficulty of preparing the Ab molecule in this state, offer an explanation for the lack of T_1 observation thus far. The quantum yield of the Z → E photosensitized photoisomerization is close to 1, while the yield of the opposite process is about 0.01.[17,52] These observations are accounted for by the fact that the lower energy S_0/T_1 crossing is on the E side and is almost degenerate with the T_1 minimum (see Figure 5).

The thermal isomerization may take place by the inversion mechanism, the adiabatic torsion mechanism on the S_0 PES and the nonadiabatic torsion mechanism via the crossing $S_0-T_1-S_0$. The latter is characterized by a lower barrier (32 kcal/mol), corresponding to the energy of the higher S_0/T_1 crossing, but requires a change in spin-multiplicity. The most efficient route at a given temperature is decided by the strength of the S_0-T_1 SO couplings.

The calculated preexponential factor for the nonadiabatic route of the thermal isomerization is similar to the rate of the $T_1 \rightarrow S_0$ isc and thus is about 10^{11} s^{-1}. This value, which is slightly lower than the typical frequency factor of an adiabatic process, is in agreement with the value of the preexponential factor obtained from the experiments.[3,4,46] The calculated activation energy of 20 kcal/mol with respect to the Z form is also consistent with the measured activation enthalpy of 22 kcal/mol.[3,4,46] Therefore, the present calculation indicates that thermal isomerization occurs by the nonadiabatic torsion mechanism and predicts kinetic parameters in agreement with the experimental results. The mechanism of the thermal isomerization of Ab has been the subject of a lively debate in the literature.[46−48,53,54] The inversion mechanism received support mainly from the observation that isomerization occurs in hindered azobenzenes.[3,48] However, as discussed above, the occurrence of isomerization observed in stilbenophanes considerably weakens

(49) Tanner, D.; Wennerstrom, O. *Tetrahedron Lett.* **1981**, *22*, 2313.
(50) Satzger, H.; Sporlein, S.; Root, C.; Wachtveitl, J.; Zinth, W.; Gilch, P. *Chem. Phys. Lett.* **2003**, *372*, 216.
(51) Lu, Y.-C.; Chang, C.-W.; Diau, E. W.-G. *J. Chin. Chem. Soc.* **2002**, *49*, 693.
(52) Jones, L. B.; Hammond, G. S. *J. Am. Chem. Soc.* **1965**, *87*, 4219.
(53) Nerbonne, J. M.; Weiss, R. J. *J. Am. Chem. Soc.* **1978**, *100*, 5953.
(54) Cimiraglia, R.; Hoffmann, H. J. *Chem. Phys. Lett.* **1994**, *217*, 430.

this argument. An alternative way to discriminate between the two mechanisms is to use liquid crystals as solvents, where the molecules are arranged in stacked layers, and solute Ab molecules, being planar, are inserted in the stacks. If the Ab molecules isomerize via a motion in the plane, they cause minimal perturbation on the solvent structure. Should the isomerization occur by torsion, the solvent layers will be disturbed. The comparison of the activation parameters measured for the thermal isomerization of Ab in isotropic and cholesteric liquid crystal solvents was found to be clearly more consistent with the torsion mechanism.[53] Thus, the torsion mechanism for the E−Z thermal isomerization appears to be supported by an experimental approach that is quite useful to elucidate reaction mechanisms.

The study of the PES and the critical geometries of the S_2 state is underway and will be presented elsewhere.

Acknowledgment. The financial support from MIUR (Project "Modellistica delle Proprietà Spettroscopiche di Sistemi Molecolari Complessi" funds ex 60% and projects "Dinamiche Molecolari in Sistemi di Interesse Chimico" and "Stereoselezione in Sintesi Organica: Metodologie ed Applicazioni" funds ex 40%), the University of Bologna (Funds for Selected Research Topics), and the FIRB projects "Microstrutture e nanostrutture a base di carbonio" is gratefully acknowledged.

Supporting Information Available: Cartesian coordinates of all the structures discussed in the text and figures displaying the molecular orbitals and wave function analysis for the three structures *Z*-Ab, CI_{tors-1}, and CI_{inv} (PDF). This material is available free of charge via the Internet at http://pubs.acs.org.

JA038327Y